



Gas Adsorption in an Isostructural Series of Pillared Coordination Cages

Journal:	<i>ChemComm</i>
Manuscript ID	CC-COM-04-2018-003216.R1
Article Type:	Communication

SCHOLARONE™
Manuscripts

Gas Adsorption in an Isostructural Series of Pillared Coordination Cages

Received 00th January 20xx,
Accepted 00th January 20xx

Eric J. Gosselin,^{†a,b} Gregory R. Lorz, ^{†a,b} Benjamin A. Trump,^c Craig M. Brown,^{c,d} and Eric D. Bloch^{*a,b}

DOI: 10.1039/x0xx00000x

www.rsc.org/

The synthesis and characterization of two novel pillared coordination cages is reported. By utilizing 1,4-diazabicyclo[2.2.2]octane (dabco) as a pillar with increased basicity as compared to pyrazine or 4,4'-bipyridine, a stable copper-based material was prepared. Extending this strategy to iron(II) afforded an isostructural material that similarly retains high porosity and crystallinity upon solvent evacuation. Importantly, the iron solid represents a rare example of porous iron paddlewheel-based metal-organic material that is stable to solvent evacuation. Neutron powder diffraction studies on these materials indicate the triangular and square windows of the cage are prime ethane and ethylene adsorption sites.

Although carboxylic acid-based porous cages have been studied for over a decade,¹ their potential utility for gas storage and separation applications has remained relatively unexplored as compared to their three-dimensional counterparts, metal-organic frameworks.² The structural relationship between these materials is striking as the former serve as discrete, molecular analogs of portions of the latter.^{3,4} Particularly, the cuboctahedral structure that paddlewheel-based isophthalic acid containing $M_{24}L_{24}$ cages adopt is present in many three-dimensional metal-organic frameworks.^{5,6,7} The high surface areas and crystallinity of these MOFs, coupled with excellent hydrogen and methane storage capacities, has motivated a number of gas adsorption and *in situ* diffraction studies.⁸ The most well-known material of this class, HKUST-1 [$Cu_3(btc)_2$; $btc^{3-} = 1,3,5$ -benzenetricarboxylate] is one of the best materials for high-pressure natural gas storage. The

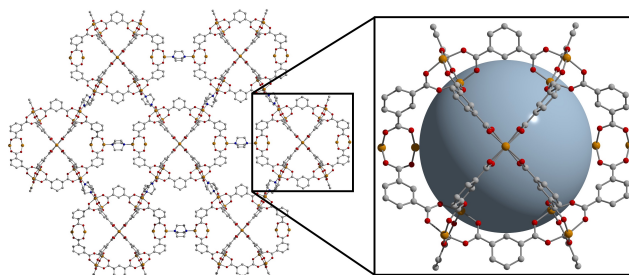


Figure 1. Structure of Fe_bdc_dabco as determined by neutron powder diffraction. Orange, red, and gray spheres represent iron, oxygen, and carbon, respectively. Hydrogen atoms and solvent molecules have been omitted. Here, cuboctahedral cages are connected in three dimensions via dabco pillaring linkers to form a framework material.

structural studies performed on this material were instrumental in elucidating its unusually high capacity.⁹

The low-dimensional nature of related porous molecular assemblies, however, makes structural characterization upon solvent removal challenging as they typically lose crystallinity with activation. Previous studies have focused on extending these cages into three-dimensional materials via the addition of pillaring ligands.¹⁰ This strategy has also been used to prepare three-dimensional metal-organic frameworks from two-dimensional structures.¹¹ However, in the case of the aforementioned cages the weak nature of the metal-pillar interaction typically results in solids that are unstable to evacuation of solvent molecules coincident with loss of crystallinity. The use of dabco, a more basic pillar consisting of aliphatic rather than aromatic nitrogen donors, was shown to engender cobalt- and zinc-based pillared cages, $M_{24}(bdc)_{24}dabco_6$, hereafter referred to as M_bdc_dabco with permanent porosity and high crystallinity upon guest evacuation.¹² We are particularly interested in studying the gas adsorption properties of porous coordination cages. However, structural characterization of these molecular compounds upon gas adsorption is particularly challenging. The aforementioned Co_bdc_dabco and Zn_bdc_dabco frameworks offer a unique opportunity to study adsorption properties across a series of materials as their syntheses can presumably be extended to a wide variety of metal cations.

Toward the synthesis of pillared coordination cages two

^a Department of Chemistry & Biochemistry, University of Delaware, Newark, DE 19716, USA. E-mail: edb@udel.edu

^b Center for Neutron Science, Department of Chemical and Biomolecular Engineering, University of Delaware, Newark, DE 19716, USA.

^c Center for Neutron Research, National Institute of Standards and Technology, Gaithersburg, MD 20899, USA.

^d Department of Chemical and Biomolecular Engineering, University of Delaware, Newark, DE 19716 USA.

[†] These authors contributed equally and are joint first authors.

Electronic Supplementary Information (ESI) available: Full synthetic procedures, powder X-ray diffraction, powder neutron diffraction, gas adsorption, isotherm fitting, infrared spectroscopy, thermogravimetric analysis, NMR spectroscopy. See DOI: 10.1039/x0xx00000x

prominent strategies have been employed. In the first, soluble cages are synthesized and isolated then pillared with pyrazine or 4,4'-bipyridine in a subsequent reaction.¹³ However, as these pillaring molecules are relatively poor ligands containing aromatic nitrogen donors, the resulting structures have proven to be unstable to solvent removal. 1,4-diazabicyclo-[2.2.2]octane (dabco) is a linear pillar analogous to pyrazine but contains aliphatic nitrogen donors with increased basicity. Accordingly, the solvothermal reaction of Cu₂OH-bdc, a highly-soluble coordination cage, with dabco in a DMF/MeOH mixture at 363 K for seven hours afforded Cu₂OH-bdc₂dabco in high yield. This material adopts the structure shown in Figure 1, as confirmed by powder neutron and X-ray diffraction. In this structure, cuboctahedra containing 12 dicopper paddlewheel units and 24 dicarboxylate bridging ligands are extended into three dimensions via bridging dabco ligands coordinated to metal cations on the exterior surface of the cage. Our attempts to extend this protocol to other copper-based assemblies were unsuccessful as these materials generally lack the solubility necessary for this approach. Additionally, cages soluble in more polar solvents such as amides typically feature bulky substituents on the 5-position of the isophthalic acid bridging ligand which are sterically incompatible with the structure depicted in Figure 1.

To address this, we modified a one-pot approach previously employed to prepare M₂bdc₂dabco (M = Co²⁺, Zn²⁺) materials.¹² For this synthesis, a Cu(NO₃)₂·N,N'-dimethylacetamide (DMA) solution containing one equivalent of isophthalic acid was pre-heated for one hour at 365 K prior to dabco addition. The presence of dabco in the initial reaction mixture prior to heating typically afforded phase-impure materials containing significant quantities of crystalline, non-pillared cages. This is likely a result of the fact that dabco is a competent base for deprotonation of isophthalic acid ligands, which has been shown to increase the rate of cage formation.¹⁴ Addition of dabco after sufficient pre-heating, followed by additional heating at 365 K for 24 hours affords the solid, Cu₂bdc₂dabco, as a phase-pure microcrystalline powder. As we are particularly interested in preparing novel coordination cage-containing materials based on first-row metals, considerable effort was put toward the synthesis of iron(II) solids. Our inability thus far to isolate functionalized Fe₂bdc₂ assemblies, however, precludes the use of a post-synthetic pillaring strategy for these materials. In the case of Fe₂bdc₂dabco, the addition of dabco to a pre-heated solution of iron chloride and isophthalic acid in DMF followed by heating at 343 K for 48 hours afforded the compound as a microcrystalline powder in moderate yield.

As X-ray-quality single crystals of the materials reported here could not be obtained, we turned to powder diffraction methods for structural determination. For this, the space group (*Fm-3m*) and initial unit cells were chosen based on the previously reported analogous cobalt and zinc materials. Precise lattice parameters and background functions were determined via Pawley refinement. The crystal structures were then solved by the global optimization method of simulated annealing in real space. As shown in Figure 1, the structures of

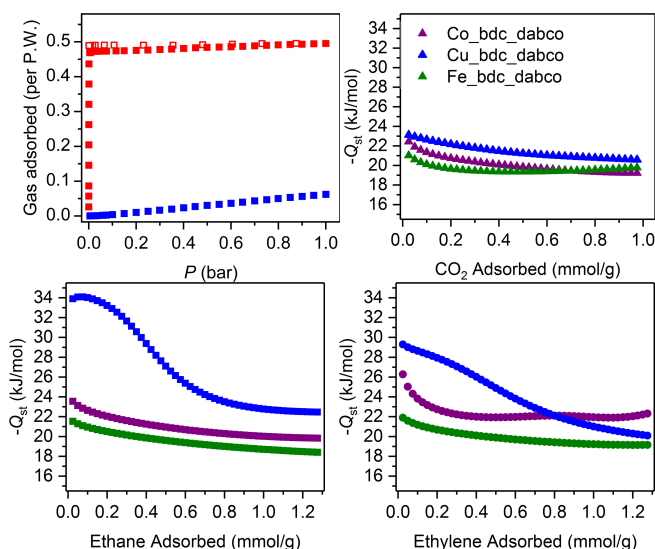


Figure 2. Adsorption of O₂ (red) and N₂ (blue) in Fe₂bdc₂dabco at room temperature (upper left). Isothermic heats of adsorption for carbon dioxide (upper right), ethane (lower left), and ethylene (lower right) for three pillared cages. For these plots of M₂bdc₂dabco, purple, green, and blue symbols represent cobalt, iron, and copper, respectively.

these materials are isostructural to the previously reported solids based on cobalt and zinc and Cu₂OH-bdc₂dabco.¹²

Previously reported M₂bdc₂dabco materials display high surface areas following exchange and evacuation of volatile solvents. For both Fe₂bdc₂dabco and Cu₂bdc₂dabco, high surface areas were obtained only after utilizing precise activation protocols. For the copper-based solid, thorough post-synthesis exchange with DMA then chloroform at elevated temperatures followed by extended drying under flowing N₂ afforded material with optimal surface areas. Rapid removal of pore-bound chloroform via dynamic vacuum routinely afforded materials with substantially decreased surface areas. For Fe₂bdc₂dabco a modified benzene freeze drying protocol was implemented.¹⁵ Ultimately, BET (Langmuir) surface areas of 1673 (2025) and 2290 (2405) m²/g were obtained for Cu₂bdc₂dabco and Fe₂bdc₂dabco, respectively. These surface areas are in good agreement with those reported for Zn₂bdc₂dabco and Co₂bdc₂dabco which displayed values of 1609 (2420) and 1802 (2722) m²/g, respectively.¹² Achieving reproducibly high surface areas was particularly challenging for Cu₂bdc₂dabco. This material, consistent with significant mass losses at low temperature in TGA experiments, has decreased thermal stability as compared to other M₂bdc₂dabco materials. Accordingly, we consistently observed decreased dabco content in the material via NMR digestion as a result of the weaker M–dabco bonds in the structure. Accordingly, typical surface areas for Cu₂bdc₂dabco were 200–300 m²/g lower than the value reported above.

As paddlewheel-based metal-organic frameworks have shown incredible utility for a variety of gas storage⁹ and separation applications¹⁶ and recent work indicating porous coordination cages show promise in this regard,¹⁷ the pillared materials reported here offer a unique opportunity to study gas storage and separation properties of porous, crystalline solids based on coordination cages. Additionally, as the first

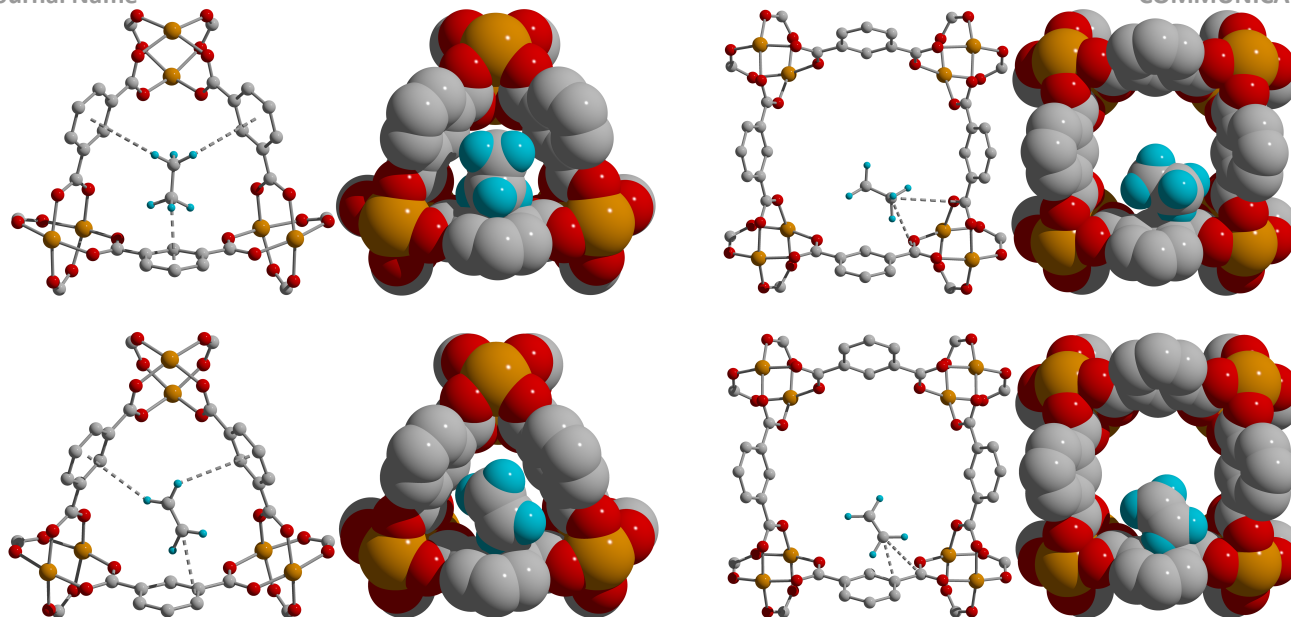


Figure 3. Structures of ethane adsorbed in the triangular (upper left) and square (upper right) windows of Fe_bdc_dabco as determined by neutron powder diffraction. Here ethane adsorbs with C-C distances of 2.78 to 3.95 Å. Ethylene adsorption sites (lower) are similar in this material with C-C distances of 2.35 to 3.26 Å.

example of an iron(II) cage-based material, we are particularly interested in studying the ability of this solid to bind oxygen for catalytic applications. As shown in Figure 2, the iron material is incredibly selective for the adsorption of O₂ over N₂ at room temperature. Specifically, O₂ uptake for Fe_bdc_dabco saturates near the value expected if half of the paddlewheels in the material bind oxygen. Nitrogen adsorption under these conditions is greatly diminished with a saturation capacity of approximately 0.05 molecules of N₂ per paddlewheel. Based on these values, the material displays an O₂/N₂ selectivity factor of 9.75.¹⁶ The steep nature of the isotherm prevented accurate fitting to calculate O₂ binding enthalpy. Accordingly, the material displays negligible O₂ uptake in subsequent measurements which indicative of irreversible binding.

Additional adsorption isotherms for CO₂, ethane, and ethylene collected on Co_bdc_dabco and the two novel materials reported here are shown in Figures S21-S32. Saturation uptakes at one bar and 298 K are relatively similar for all three materials across the series of adsorbates. However, the copper material displays the highest saturation uptakes for all gases measured, despite its diminished surface. Accordingly, isosteric heats of adsorption calculated from temperature dependence of gas uptake indicate that the copper material displays increased gas binding enthalpies at low coverage. Infrared spectra for activated materials indicate the presence of significant amounts of metal-coordinated amide solvent for both the cobalt and iron materials. Attempts to remove metal-bound DMF by heating at elevated temperatures resulted in significantly decreased surface areas. In these pillared structures, loss of metal-bound solvent coincides with loss of dabco from the structure. Although the temperatures at which this was observed for the iron and cobalt materials resulted in significantly diminished surface areas, the copper structure is stable to removal of approximately 25 % of the coordinated DMF and dabco. This has the effect of increasing the number of higher-enthalpy

binding sites available as metals on both the interior and exterior of a given cage become accessible to gas molecules. Accordingly, in the copper material the low coverage isosteric heat of ethane adsorption is approximately -33 kJ/mol compared to -30 kJ/mol for ethylene. At low coverage, the analogous iron framework displays binding enthalpies of just -22 kJ/mol for both gases. This value is in agreement with those previously seen for a metal-organic framework lacking open metal sites.¹⁸

To gain insight into the mechanism of ethane and ethylene adsorption in these materials, we turned to neutron powder diffraction. This has previously been used to reveal CD₄, D₂, and C₂D₂ binding in metal-organic frameworks featuring cuboctahedral building units in their structures. In these materials, the open metal cation sites are typically the preferentially populated sites at low coverage.¹⁹ However, in the materials presented here, the pillaring dabco molecule is coordinating to the exterior metal cation site with significant occupancy of coordinated DMF on the interior site. Refinements against powder patterns collected on Fe_bdc_dabco in the presence of either of these hydrocarbons reveal similar gas adsorption sites for ethane and ethylene. Here, the triangular window on the polyhedron is preferentially occupied by the hydrocarbon molecules as a result of favorable D-arene interactions. However, the similar polarizabilities and kinetic diameters of these two molecules, which manifests in similarity of adsorption enthalpies, also results in similarities in adsorption sites with ethylene interacting with the pore surface in a similar manner. These results, taken with our previous work indicating chromium(II)-based ^tBu-bdc materials are poorly suited for the separation of paraffin/olefin molecules,¹⁷ suggest new structure types must be developed to achieve appreciable separation for these types of gas mixtures with porous molecular assemblies.

The results presented here demonstrate that pillaring copper-based porous molecular assemblies with sufficiently

basic ligands affords materials that both display permanent porosity upon evacuation and retain high crystallinity. Additionally, a one-pot pillaring strategy has been employed to prepare a novel iron(II)-based metal-organic material. Importantly, this material represents a rare example of an iron paddlewheel-based porous solids that is stable to evacuation.²⁰ Accordingly, they display selective O₂/N₂ adsorption at room temperature. We are currently studying the oxidized material for selective O-atom transfer reactivity. Additional future work will focus on a route to remove dabco from these three-dimensional structures to afford discrete cages.

E.D.B. is grateful to the University of Delaware for generous start-up funds. This manuscript was prepared under cooperative agreement # 70NANB12H239 from NIST, U.S. Department of Commerce. We acknowledge the support of the National Institute of Standards and Technology, U.S. Department of Commerce, in providing the neutron facilities used in this work. This research used resources of the Advanced Photon Source, a U.S. Department of Energy (DOE) Office of Science User Facility operated for the DOE Office of Science by Argonne National Laboratory under Contract No. DE-AC02-06CH11357. We thank the staff of 17-BM for help with synchrotron X-ray data collection. B.A.T. recognizes the National Academies/National Research Council for his Postdoctoral Fellowship.

Conflicts of interest

There are no conflicts to declare.

References

- M. Eddaoudi, J. Kim, J. B. Wachter, H. K. Chae, M. O'Keeffe, O. M. Yaghi, *J. Am. Chem. Soc.*, 2001, **123**, 4368; A. C. Sudik, A. R. Millward, N. W. Ockwig, A. P. Cote, J. Kim, O. M. Yaghi, *J. Am. Chem. Soc.*, 2005, **127**, 7110; Y. Ke, D. J. Collins, H. -C. Zhou, *Inorg. Chem.*, 2005, **44**, 4154; M. D. Young, Q. Zhang, H. -C. Zhou, *Inorg. Chim. Acta.*, 2015, **424**, 216; S. Furukawa, N. Horiki, M. Kondo, Y. Hijikata, A. Carne-Sanchez, P. Lerpent, N. Louvain, S. Diring, H. Sato, R. Matsuda, R. Kawano, S. Kitagawa, *Inorg. Chem.*, 2016, **55**, 10843; J. M. Teo, C. J. Coghlan, J. D. Evans, E. Tsvion, M. Head-Gordon, C. J. Sumby, C. J. Doonan, *Chem. Commun.*, 2016, **52**, 276.
- M. Eddaoudi, J. Kim, N. Rosi, D. Vodak, J. Wachter, M. O'Keeffe, O. M. Yaghi, *Science*, 2002, **295**, 469; S. Kitagawa, R. Kitaura, S. -I. Noro, *Angew. Chem. Int. Ed.*, 2004, **43**, 2334; G. Férey, *Chem. Soc. Rev.*, 2008, **37**, 191; B. Chen, X. Xiang, G. Qian, *Acc. Chem. Res.*, 2010, **43**, 1115.
- S. S. -Y. Chui, S. M. -F. Lo, J. P. H. Charmant, A. G. Orpen, I. G. Williams, *Science*, 1999, **283**, 1148; M. Kramer, U. Schwarz, S. Kaskel, *J. Mater. Chem.*, 2006, **16**, 2245; J. I. Feldblyum, M. Liu, D. W. Gidley, A. J. Matzger, *J. Am. Chem. Soc.*, 2011, **133**, 18257; S. Krause, V. Bon, I. Senkovska, U. Stoeck, D. Wallacher, D. M. Tobbens, S. Zander, R. S. Pillai, G. Maurin, F. -X. Coudert, S. Kaskel, *Nature*, 2016, **532**, 348.
- J. -R. Li, A. A. Yakovenko, W. Lu, D. J. Timmons, W. Zhuang, D. Yuan, H. -C. Zhou, *J. Am. Chem. Soc.*, 2010, **132**, 17599.
- D. Yuan, D. Zhao, H. -C. Zhou, *Inorg. Chem.*, 2011, **50**, 10528.
- Y. Yan, S. Yang, A. J. Blake, W. Lewis, E. Poirier, S. A. Barnett, N. R. Champness, M. Schroder, *Chem. Commun.*, 2011, **47**, 9995.
- O. K. Farha, C. E. Wilmer, I. Eryazici, B. G. Hauser, P. Parilla, K. O'Neil, A. A. Sarjeant, S. T. Nguyen, R. Q. Snurr, J. T. Hupp, *J. Am. Chem. Soc.*, 2012, **134**, 9860.
- Y. Yan, D. I. Kolokolov, I. da Silva, A. G. Stepanov, A. Blake, A. Dailly, P. Manuel, C. C. Tang, S. Yang, M. Schroder, *J. Am. Chem. Soc.*, 2017, **139**, 13349.
- J. Getzschmann, I. Senkovska, D. Wallacher, M. Tovar, D. Fairen-Jimenez, T. Duren, J. M. van Baten, R. Krishna, S. Kaskel, *Microporous Mesoporous Mater.*, 2010, **136**, 50; H. Wu, J. M. Simmons, Y. Liu, C. M. Brown, X. -S. Wang, S. Ma, V. K. Peterson, P. D. Southon, C. J. Kepert, H. -C. Zhou, T. Yildirim, W. Zhou, *Chem. Eur. J.*, 2010, **16**, 5205; Y. -P. Chen, Y. Liu, D. Liu, M. Bosch, H. -C. Zhou, *J. Am. Chem. Soc.*, 2015, **137**, 2919; Z. Hulvey, B. Vlaisavljevich, J. A. Mason, E. Tsvion, T. P. Dougherty, E. D. Bloch, M. Head-Gordon, B. Smit, J. R. Long, C. M. Brown, *J. Am. Chem. Soc.*, 2015, **137**, 10816.
- H. -N. Wang, X. Meng, G. -S. Yang, X. -L. Wang, K. -Z. Shao, Z. -M. Su, C. -G. Wang, *Chem. Commun.*, 2011, **47**, 7128; H. -N. Wang, F. -H. Liu, X. -L. Wang, K. -Z. Xhao, Z. -M. Su, *J. Mater. Chem. A.*, 2013, **1**, 13060.
- O. Kozachuk, K. Khaletskaya, M. Halbherr, A. Betard, M. Meilikhov, R. W. Seidel, B. Jee, A. Poppl, R. A. Fischer, *Eur. J. Inorg. Chem.*, 2012, 1688; H. Jasuja, K. S. Walton, *Dalton Trans.*, 2013, **42**, 15421; O. Karagiari, W. Bury, D. Fairen-Jimenez, C. E. Wilmer, A. A. Sarjeant, J. T. Hupp, O. K. Farha, *Inorg. Chem.*, 2014, **53**, 10436; A. Schneemann, V. Bon, I. Schwedler, I. Senkovska, S. Kaskel, R. A. Fischer, *Chem. Soc. Rev.* 2014, **43**, 6062;
- H. Chun, *J. Am. Chem. Soc.*, 2008, **130**, 800; H. Chun, H. Jung, J. Seo, *Inorg. Chem.*, 2009, **48**, 2043.
- J. -R. Li, D. J. Timmons, H. -C. Zhou, *Inorg. Chem.*, 2009, **131**, 6368.
- J. -R. Li, H. -C. Zhou, *Nat. Chem.*, 2010, **2**, 893.
- L. Ma, A. Jin, Z. Xie, W. Lin, *Angew. Chem. Int. Ed.*, 2009, **48**, 9905.
- L. J. Murray, M. Dinca, J. Yano, S. Chavan, S. Bordiga, C. M. Brown, J. R. Long, *J. Am. Chem. Soc.*, 2011, **133**, 18257; C. R. Wade, M. Dinca, *Dalton Trans.*, 2012, **41**, 7931; B. Supronowicz, A. Mavrandonakis, T. Heine, *J. Phys. Chem. C*, 2013, **117**, 14570.
- J. Park, Z. Perry, Y. -P. Chen, J. Bae, H. -C. Zhou, *ACS Appl. Mater. Interfaces*, 2017, **9**, 28064; G. R. Loring, B. A. Trump, C. M. Brown, E. D. Bloch, *Chem. Mater.*, 2017, **29**, 8583.
- M. T. Luebbers, T. Wu, L. Shen, R. Masel, *Langmuir*, 2010, **26**, 11319.
- S. Xian, W. Zhou, J. M. Gallegos, Y. Liu, B. Chen, *J. Am. Chem. Soc.*, 2009, **131**, 12415; H. Wu, J. M. Simmons, Y. Liu, C. M. Brown, X. -S. Wang, S. Ma, V. K. Peterson, P. D. Southon, C. J. Kepert, H. -C. Zhou, T. Yildirim, W. Zhou, *Chem. Eur. J.*, 2010, **16**, 5205.
- A. Fateeva, J. Clarisse, G. Pilet, J.-M. Greneche, F. Nouar, B. K. Abeykoon, F. Guegan, C. Goutaudier, D. Luneau, J. E. Warren, M. J. Rosseinsky, T. Devic, *Cryst. Growth. Des.* 2015, **15**, 1819.